Nanoscale

PAPER

View Article Online
View Journal | View Issue

Cite this: *Nanoscale*, 2018, **10**, 12797

Towards personalised rapid label free miRNA detection for cancer and liver injury diagnostics in cell lysates and blood based samples†

James Duffy, [a] Francesco Padovani, [a] Giulio Brunetti, [a] Peter Noy,[b] Ulrich Certa[b,c] and Martin Hegner *[a]

Advances in prevention, diagnosis and therapy are coupled to innovation and development of new medical tools, leading to improved patient prognosis. We developed an automatic biosensor platform that could provide a non-invasive, rapid and personalised diagnosis using nanomechanical cantilever sensors. miRNA are involved in gene expression and are extractable biomarkers for multiple diseases. We detected specific expression patterns of miRNA relevant to cancer and adverse drug effects directly in cell lysates or blood based samples using only a few microliters of sample within one hour. Specific miRNA hybridisation to the upper cantilever surface induces physical bending of the sensor which is detected by monitoring the position of a laser that reflects from the sensors surface. Internal reference sensors negate environmental and nonspecific effects. We showed that the sensitivity of label free cantilever nanomechanical sensing of miRNA surpasses that of surface plasmon resonance by more than three orders of magnitude. A cancer associated miRNA expression profile from cell lysates and one associated with hepatocytes derived from necrotic liver tissue in blood-based samples has been successfully detected. Our label free mechanical approach displays the capability to perform in relevant clinical samples while also obtaining comparable results to PCR based techniques. Without the need to individually extend, amplify or label each target allowing multitarget analysis from one sample.

Received 3rd May 2018,
Accepted 13th June 2018

DOI: 10.1039/c8nr03604g

rsc.li/nanoscale

Introduction

MicroRNAs (miRNA, miR) are post transcriptional, sequence specific gene expression regulators.[1] These molecules are 21–25 nucleotides in length. Recent breakthroughs in understanding of the essential roles of regulatory miRNAs have created new opportunities in the field of direct disease detection. Circulation and stability in serum,[2] resistance to endogenous ribonuclease activity[3] and presence in cell secreted particles including exosomes and apoptotic bodies[4,5] make miRNA a promising biomarker. However, the short length of individual miRNA results in traditional detection methods such as PCR based approaches requiring modification, molecular extension, labelling and amplification of the target. Profiling miRNA expression patterns has tremendous potential for the diagnosis of a broad range of diseases including cancer,[6] blood stream infections,[7] cardiovascular disorders,[8] and Alzheimer's.[9] They also indicate side effects of therapeutic drugs.[10]

Drug induced liver injury (DILI) accounts for over 50% acute liver failure in the USA, with 39% of these cases attributed to Acetaminophen (APAP) overdose.[11] Also liver adverse effects are the most common cause of drug withdrawal from the market.[12] Acute overdose of the analgesic APAP results in hepatocyte death with release of cellular contents including miRNA.[13] Colorimetric serum measurement of alanine aminotransferase (ALT) is the current clinical standard for DILI diagnosis. Recent research in ALT detection has focussed on electrochemical methods which struggle with interference from biomolecules reducing signal resolution, and false positives.[14] Furthermore ALT is not liver specific. Muscle injury has been shown to increase blood ALT levels by up to 140%.[15] Hence additional biomarkers with higher specificity, such as miRNA, would assist in eliminating false positives.

Cancer accounts for 25% of deaths in developed countries.[16] Central to successful treatment of cancer is early and accurate diagnosis. Detecting tumour derived miRNA

[a]*Centre Centre for Research on Adaptive Nanostructures and Nanodevices (CRANN), School of Physics, Trinity College Dublin, Dublin 2, Ireland. E-mail: martin.hegner@tcd.ie*
[b]*F. Hoffmann-La Roche Ltd., Pharma Research and Early Development, Discovery Technologies, 4070 Basel, Switzerland*
[c]*F. Hoffmann-La Roche Ltd., Global Non-clinical Safety, Molecular Toxicology, 4070 Basel, Switzerland*

†Electronic supplementary information (ESI) available. See DOI: 10.1039/c8nr03604g

could provide accurate disease state information. This can be attributed to the following factors. Firstly, irregular miRNA levels have been described in tumours as well as established cancer cell lines.[17] Second, tumour cells have been shown to release subcellular particles known as exosomes into circulation.[18] Thirdly, the miRNA expression profiles of these circulating exosomes are equivalent to that of the present tumour cells.[19] There is no current gold standard for investigating miRNA expression, however real-time quantitative reverse transcription PCR (qRT-PCR) provides the highest sensitivity. PCR based miRNA analysis techniques are based on whether target molecules are reliably extended, labelled and amplified. These processes can introduce a bias in the analysis of miRNA expression levels. Furthermore assay conditions require adaptation and optimisation for each miRNA target thereby limiting feasibility of multiparallel quantification. In addition there is not yet a standardised method for isolation of exosomal miRNA from serum.[20] The diagnostic marker miRNAs chosen for this study are DILI specific miR-122 and liver cancer indicative miR-148b and miR-192 that have been established as relevant biomarkers using qRT-PCR in several clinical studies.[21–25]

The assay presented here enables profiling of multiple miRNA from small sample volumes without modification or amplification. Signal generation relies on specific nucleic acid hybridisation occurring in a densely packed, surface bound nucleic acid probe (complimentary to target miRNA sequence) monolayer on one side (gold coated top side) of a microcantilever. Hybridisation imparts a differential surface stress between the top and bottom surface due to steric hindrance and electrostatic repulsion between neighbouring surface bound molecules.[26,27] This causes the cantilevers to deflect which is detected by monitoring the position of a laser reflecting off the upper gold coated cantilever surface. Fig. 1 shows a representation of the mechanical cantilever array approach (not drawn to scale). Sensitivity in competitive nucleic acid environments of 10 fM has been reported.[28] Single nucleotide mismatches have also been detected.[29] *In situ* reference sensors were used to negate environmental and nonspecific effects.[28,30] A label free piezoelectric cantilever miRNA assay with attomolar sensitivity has been reported, however without *in situ* reference controls.[31]

Other comparable techniques such as surface plasmon resonance (SPR) which optically detects local changes in the index of refraction upon biomolecular attachment to a metal surface[32] requires labelling with DNA-linked gold nanoparticles to reduce the lower limit of detection.[33] Localised surface plasmon resonance (LSPR) using gold nanocubes has reported miRNA detection sensitivity of 5 pM in serum.[34] However this single channel measurement was performed in 2% fetal bovine serum and probed for one single miRNA only. Branched DNA assays or DNA ELISA require no target amplification, instead they require capture probes, detection probes or label extenders. These can be costly and time consuming. Specificity is also reduced as nucleotides from the target are used for label attachment and hence not available for detection. Here we present a prototype device capable of detecting multiple miRNA signatures from clinically relevant samples without amplification, labelling or isolation procedures. Measurements are directly conducted in Acetaminophen DILI blood based samples from rats or cell lysates from human hepatocellular carcinoma (HCC) cell line.

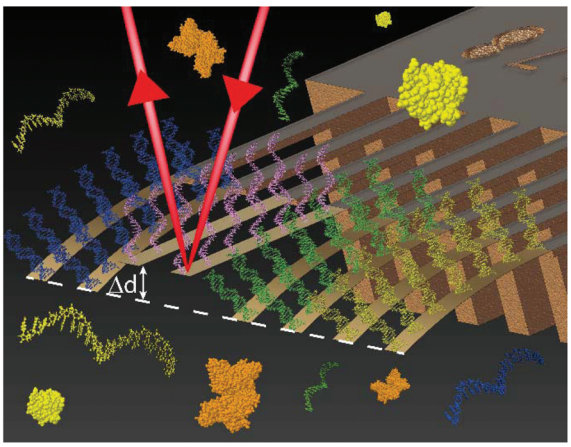

Fig. 1 Illustration of target binding on the cantilever array surface. Perspective is from inside the fluidic chamber. The laser from the optical beam read out detection method is shown reflecting away from a cantilevers surface, out of the chamber and towards the detector. Differential deflection (Δd) arise between the *in situ* reference probes (pink) and target sensitive probes (blue, green and yellow), four times two sensors each. Targets are captured *via* specific nucleic acid hybridisation on the densely packed oligonucleotide receptor layer on the top side of the sensor array. Steric hindrance of the hybridised targets on the higher populated probe sensors build-up of stress and cause a downward bending. Low concentration of proteins, globulin (yellow) and albumin (orange), are also depicted to indicate measurements in serum or plasma. The dimensions of the objects shown is not drawn to scale.

Results and discussion

Comparative study surface plasmon resonance assay *versus* cantilever array assay

Biacore's surface plasmon resonance system, the gold standard for label-free quantitative biomolecular interaction analysis, was used as a reference parallel to the cantilever array technology. We compared the sensitivity of the two fundamentally different systems, in order to further support the interpretation of our results. To compare the methods, we utilized SPR chips with blank gold surfaces that were functionalised with oligonucleotides. A dose response curve was plotted summarizing all SPR measurements (blue curve in Fig. 2). We also plotted an overlay of the dose response curve from the cantilever experiment for the subsequent detection of miR-122 in Me15 cell lysate (red curve). We recorded a dose response curve with known concentrations of spike-in miRNA target in control Me15 cell lysate as reference (Me15 does not over express miR-122[35]) to enable correlation of nanometer deflection to target concentration. Example data from the series of

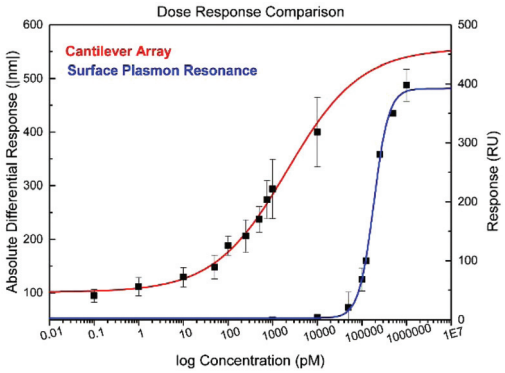

Fig. 2 Dose response comparison cantilever array *versus* SPR. Summarised SPR hybridisation data obtained using Biacore sensor chip functionalised with 1 μM thiolated probe for 1 hour. A logistic model was applied and a sigmoidal fit plotted. SPR measurements had to be conducted in pure nucleic acids spike in solutions as measurements in cell lysate were not possible due to a complete masking of the miRNA concentration signals by the lysate proteins. Error bars include chip to chip variabilities and intra chip results. Cantilever array annealing data obtained from ten miRNA target spike-in concentration experiments in Me15 cell lysate background in flow-through conditions (see Methods). Error bars are calculated using the standard deviation from three measurements. As observed the dynamic range of the cantilever based technology is larger than the one from the surface plasmon technology.

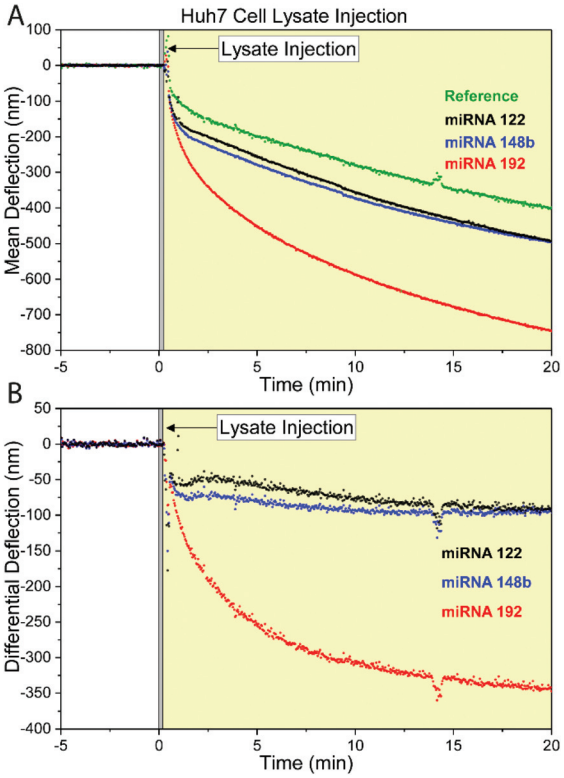

Fig. 3 Huh7 cell lysate injection. A: Mean deflection of two cantilevers per probe group (see Materials and methods). At 14 minutes there is a deviation in the reference sensor data due to cell lysate particles scattering the laser of the optical read out system. This artefact carries into the differential signal. The grey area represents an injection of 38 μl of diluted cell lysate at 150 μl min^{-1}. The yellow area indicates the incubation time after the injection, liquids stop moving and the sample interacts with the nanomechanical sensor array. Fluidic events are identical between both plots in this figure. B: Differential deflection obtained by subtracting the reference response from each of the miRNA probe responses, revealing the mechanical signal rising from the specific interaction between miRNA and the sensor biolayer. The strongest hybridisation signal is produced by the miR-192 probe. While the probes corresponding to miR-122 and 148b exhibit a diminished annealing signal. The reference probe, originating from the firefly luciferase gene, displays the smallest response. These findings match the reported RT-PCR miRNA expression studies in hepatocellular carcinoma.[21–23] Providing that the differential signal is surpassing the signal-to-noise level silicon underside passivation is not required for cantilever biological ligand detection.[37]

experiments used to produce Fig. 2 are available in the ESI (Fig. S2 and S3†).

Direct measurements in cell lysate

We performed cantilever array experiments that explored the differential detection of several miRNA targets in cell lysates simultaneously. The sensor array was functionalised with ssDNA probes complimentary to specific miRNAs expressed variably in Huh7 cells from human liver carcinoma. Functionalisation was done in pairs of sensors as described in the material and methods section. Of the eight sensors we used two reference sensors positioned in 1 and 3 and then a pair of miR-192, miR-148b and miR-122 probes in position 2, 4, 5, 7, 6 and 8 respectively. Upon diluted cell lysate injection all cantilevers were deflected downwards up to 750 nm (Fig. 3A), due to specific target annealing despite high levels of serum proteins. This response is typical of cantilever surface short nucleic acid hybridisation in complex backgrounds of total cellular RNA.[28] Sensors targeting miR-192 showed the greatest hybridisation response of ~750 nm while miR-122 and miR-148b displayed a lesser response of ~600 nm. Reference sensors gave the weakest response, caused solely by nonspecific interaction between the sensor surfaces and the cell lysate molecules, by applying a differential analysis this reaction can be disregarded. Reference sequence used here was a segment from the firefly luciferase gene, *Luc*.[36] The differential analysis in Fig. 3B is emphasizing the specific contribution of the nucleic acid hybridization. As expected miR-192 is present at higher levels than miR-122 and miR-148b. In HCC miR-192 has been reported as overexpressed[21] while miR-122 and miR-148b have been reported as down regulated *via* PCR based techniques.[22,23] It is possible to convert these deflection values into miRNA concentrations as Fig. 2 can be used for an estimation. Cantilever response equilibria for each target concentration are displayed in Fig. 2. These experiments were conducted using continuous flow of 600 μl of target. Equilibrium was regularly reached after ~400 μl. Individual measurements are shown in the ESI.† We can detect if over expression has occurred, by comparing the responses of the target sensitive sensors with each other and with the reference sensor. Rinsing of the chamber (data not shown) lessens the differential response. Continuous flow experiments probing for miR-122

in positive Huh7 and negative Me15 cell lysate (Fig. S1†) are available in the ESI.†

Drug induced liver injury: miRNA release analysed in blood plasma or serum from rats

To validate our method we performed measurements of specific miRNA directly in blood plasma or serum. miR-122 is specifically expressed and highly abundant in the human liver[24] and conserved between vertebrate species.[25] Exposing the array to diluted EDTA-treated plasma imparts surface stresses that leads to an overall bending cantilever (Fig. 4A). We observed a convolution of the environmental effects[38] but the underlying biological specific response remains detectable.[28,29] As seen in Fig. 4A stress in the sensors induces an absolute deflection of up to 700 nm due to nonspecific adsorption of proteins onto the bare silicon of the cantilevers, forcing the cantilevers to bend.[39] Within 10 minutes the reference sensor coated with miR-27a probe oligonucleotides is seen ~100 nm below target sensitive sensors. Differential readout (Fig. 4C) reveals the specific interaction of the targets to the sensor interface.[40] At the end of incubation both miR-192 and 148b remain 100 nm above the reference. Examining Fig. 4C displays the miR-122 sensor sitting ~190 nm above the reference sensor, indicating that miR-122 is present at higher levels than miR-192 and 148b as a result of DILI. Similar results have been reported using PCR based methods,[41] showing that DILI *via* Acetaminophen overdose in rats leads to increased levels of miR-122 and 192 in circulation. While miR-148b, which is down regulated in hepatocyte carcinomas,[42] here it gives a higher hybridisation signal (Fig. 4C) than the chosen reference miR-27a, a known human breast tissue oncogenic miRNA.[43] The rate of hybridisation and hence deflection change slows down as the number of unbound probes is reduced (Fig. 4A). Introducing serum samples from non-treated rats leads to the development of less defined differential mechanical response due to the lack of miRNA in the protein rich environment (Fig. 4B). Target sensitive sensors can be seen crossing over each other within the first 10 minutes. This nonspecific response results from drift caused by serum proteins interacting with hydrophobic regions of the ssDNA biolayer and the cantilevers exposed surfaces. Diagnostic evaluation can be concluded within a time frame of 20 minutes, however final saturation is reached in 1 hour. Thus, no biologically specific response is obtained as compared to the APAP treated rat plasma which contains clotting factors, serum proteins and liver specific miRNA. Also Fig. 4B shows no change in kinetics as there is no miRNA present to bind to available surface probes. Following the buffer rinse of the chamber all sensors can be seen relaxing, due to the removal of some non-specifically adsorbed proteins. Noise fluctuations, caused by optical interference of the serum protein and particles with the laser beam, also return to normal after the buffer rinse (data not shown).

Discussion

The assay demonstrated the ability to directly detect miRNA at significantly lower levels than SPR and document that the results compare with PCR experiments in clinical settings. Furthermore detection of DILI and HCC relevant miRNA from biological samples without labelling or amplification using small samples volumes was also achieved. Comparing the techniques (SPR and the cantilever array) side by side we see differences in the two assay types (Fig. 2). This result leads to a better understanding in terms of sensor response such as dynamic range and sensitivity. For each concentration, the corresponding result was plotted (deflection in [nm] for cantilever and shift of refractive index in [RU] for SPR). From the

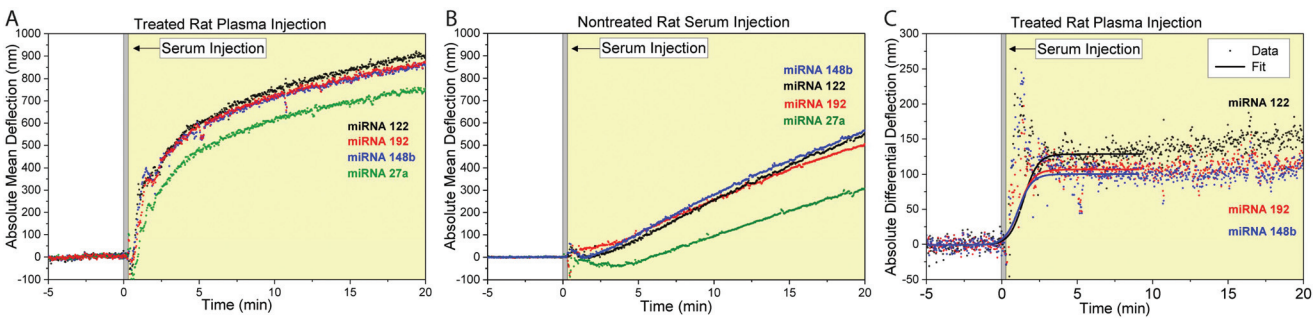

Fig. 4 APAP exposed Rat EDTA-treated plasma and non-treated rat serum injection. A: Absolute mean deflection of two cantilevers per probe group in response to injection of 38 μl of diluted EDTA treated plasma from Acetaminophen treated rats at 150 μl min^{-1} (grey area). Absolute deflection values are plotted as blood coagulation proteins in plasma affect mechanical signal directionality. Fluidic events are identical between all plots contained in this figure. The yellow area represents the incubation time where the miRNA can interact with the cantilever array surface biolayer. B: Absolute mean deflection of two cantilevers per probe group upon injection of diluted serum from non-treated rats. As no liver specific miRNA occurring from hepatocyte cell death are present in 'non-treated' serum we see a nonspecific evolution of the deflection signal. Generated by serum proteins interacting with the sensor interfaces. Thus, no change in kinetics is observed as target molecules are not present to occupy sensor bound probes. C: Treated rat plasma differential deflection. A differential deflection sensogram produced by subtracting the reference sensor response (miR-27a, human breast tissue oncogenic miRNA) from the target sensitive probe response. This permits investigation of the interaction between the miRNA released *via* hepatocyte cell death, induced *via* Acetaminophen overdose, and the surface bound probes in a protein rich environment. Liver specific miR-122 hybridisation gives the greatest response. While miR-192 and 148b likewise yield a differential signal. Indicating the presence of liver associated miRNA in serum post drug induced liver injury.

curve representing the cantilever array measurements (Fig. 2) we can estimate the resulted response in an experiment to miRNA concentration in cell lysates. Our SPR data was in perfect range to previously reported assays.[44,45] SPR measurements had to be conducted in pure nucleic acids spiked in buffer solutions as measurements in cell lysate were not possible due to a complete masking of the miRNA concentration index of refraction signals at the interface by the lysate molecules. Our nanomechanical assay utilising soft cantilevers structures shows an increased dynamic range and limit of detection (more than three orders of magnitude) compared to SPR. The surface stress based mechanical response, the compliance of the soft sensors (0.004 N m^{-1}) and nanometer resolution of the optical read out system delivers increased sensitivity and performance.

Critical to the interpretation of the nanomechanical response is thorough data analysis and internal reference controls. Normalisation and averaging of a few mechanical sensor responses measured simultaneously in the assay chamber is essential, as is the knowledge of the source (organism type) of the sample being analysed, this could alter the specific sequence of the miRNA slightly (see Table 1). Cantilever upper surface short nucleic acid hybridisation in biological environments (cell lysates) results in a downward deflection of the sensors. In Fig. 3A all sensors exhibit downward deflection post sample injection, indicating that nucleic acid duplex formation dominates the sensor response in lower protein concentration samples (20 times lower than blood based samples). Differential signal (Fig. 3B) reveals miR-192 is present at higher levels than miR-122 and miR-148b.

The absolute deflection values for the DILI study was plotted (Fig. 4A–C). Detection of miRNA in blood-based samples produces a specific differential response. The hydrophilic SiO_2 underside of the cantilever interacts differently with proteins than the charged topside nucleic acid probe layer. The random evolution of the nanomechanical response in non-treated rat serum in Fig. 4B contrasts Fig. 4A and indicates an overall average offset of the target sensors of 300–550 nm that stems from the unspecific interactions on the sensors surface. However, this response lacks the change in kinetics which is seen in other experiments where miRNAs (Fig. 4A). Sample from a healthy organism contains significantly less freely circulating nucleic acid.[46] Hybridisation prevents excessive nonspecific plasma or serum protein adsorption within the probe layer, leading to a stable differential response (Fig. 4C). We believe the 20 fold higher protein concentration in plasma to be the reason for tensile stress dominating the cantilever response in blood based samples and the reduced differential signal when compared to measurements in cell lysates (Fig. 3B). It is important to note that the signal response represented in Fig. 2 for SPR were obtained in pure target nucleic acid environments and whereas the cantilever technology assays were conducted in a heterogeneous cell lysate background containing proteins, indicating the superiority of the nanomechanical based direct detection assay.

The current gold standard for the detection of several miRNA targets from blood based samples is qRT-PCR. We establish that a nanomechanical assay can provide quantitative analysis of an expression pattern directly in a one-shot reaction without purification, amplification or labelling. Therefore allowing miRNA expression profiling from a sample in one single experiment. To enhance the differential signal from blood-based samples denaturation of native ribonucleoprotein, followed by protein removal would reduce nonspecific drift response as seen in Fig. 4B, allowing an enhanced differential signal to develop as seen in Fig. 3B.

Future work will focus on expanding the assay, redesigning the sensor chip by increasing the number of miRNA sensors and to obtain a disposable self-contained and ready-to-use chip cartridge. We will explore the value of high affinity nucleic acid analogues as miRNA probes.[47] The results presented here describe a medical device prototype that performs automated label free nanomechanical measurements of miRNA. Validation in a clinical setting is planned and risk analysis will have to be performed and documented before medical device approval for a class I device can be sought.

Materials and methods

Details of the fully automated experimental setup can be found in Walther *et al.*[48] In short, an array consisting of 8 cantilevers (two per target) is fixed in a microfluidic measurement chamber of 8 μl volume. This chamber allows fluids to

Table 1 Sequence and citations for the nucleic acid probes used for cancer and drug induced liver injury indicative miRNA detection

Reference miRNA	Sequence	Citation
Luc (from firefly)	HS-$(CH_2)_6$-CTT ACG CTG AGT ACT TTG A	Ravon *et al.* (2012)[36]
miR-27a compliment	HS-$(CH_2)_6$-TGC TCA CAA GCA GCT AAG CCC T	Li *et al.* (2010)[43] Landgraf *et al.* (2007)[24]
Cancer or toxicology relevant miRNA		
miR-122 compliment	HS-$(CH_2)_6$-CAA ACA CCA TTG TCA CAC TCC A	Coulouarn *et al.* (2009)[23] Landgraf *et al.* (2007)[24]
miR-192 compliment	HS-$(CH_2)_6$-GGC TGT CAA TTC ATA GGT CAG	Lin *et al.* (2015)[21] Landgraf *et al.* (2007)[24]
miR-148b compliment (rat)	HS-$(CH_2)_6$-CCT GAG TGT ATA ACA GAA CTT C	Linsen *et al.* (2010)[25]
miR-148b compliment (human)	HS-$(CH_2)_6$-GCC TGA GTG TAT AAC AGA ACT T	Arrese *et al.* (2015)[42] Landgraf *et al.* (2007)[24]

be exchanged and samples to be introduced *via* a micro-dispensing valve. A heating element induces a heat pulse that enables normalisation of the mechanical motion of the cantilever array sensors. This heating element is situated beneath the measurement chamber. Optical beam deflection readout method is employed to measure cantilever deflection. The laser is mounted on two automatic stages (M-122.2DD and M-110.1DG, Physik Instrumente Ltd, Bedford, England). Allowing the laser spot to travel between and along all eight cantilevers. Enhancements made to the device mentioned above are listed in ESI.†

Cantilever preparation

Cantilever arrays containing silicon 8 cantilevers were acquired from IBM Zurich. The cantilevers are 500 μm in length, 100 μm in length and 500 nm in thickness and their pitch is 250 μm (spring constant 0.004 N m^{-1}). Arrays were cleaned with immersions in various solvents SPR followed by plasma cleaning as described by Padovani *et al.*[49] Once cleaned, the topside of the cantilevers were coated in a vacuum deposition tool (Temescal, Scotech UK) with 3 nm titanium and 23 nm gold. ssDNA probes containing a $(CH_2)_6$ linker modifications at the 5′ position were obtained from Microsynth (Balgach, Switzerland). Probe solutions of 20 μM in 50 mM triethylammonium acetate (Sigma Aldrich, Ireland) were used to functionalise the sensors with specific nucleic acid sequences that are complimentary to the individual miRNA targets. Functionalisation was performed using the glass capillary method for 20 minutes.[50] Reference and target sensitive cantilevers are located within the same array of sensors. As shown in Fig. 1 the functionalisation of the sensor was conducted to have a pattern of four miRNA sequences on two cantilevers respectively. After functionalisation, the array was rinsed twice and stored in Dulbecco's Phosphate Buffered Saline with calcium chloride and magnesium chloride (DPBS+, Sigma Aldrich) over night at room temperature in DPBS+.

As shown in the Table 1, we chose two different probe sequences to allow for an internal nanomechanical reference. The sequence from firefly *Luc*[36] for the SPR study and the cell lysate experiments and miR-27a[43] (overexpressed in breast carcinoma tissue) has been used in the rat sample analysis. The sequences of miR-148b from rat and human differ in one nucleotide only.

Measurement protocol

Fig. 5 shows the standardised work flow for nanomechanical measurements. To allow internal normalisation and quality control of the nanomechanical bending of the sensors we firstly applied a heat pulse of 2 °C. The heat pulse, delivered by a peltier element situated beneath sensor array, causes the cantilevers in the arrays to deflect downwards by several hundred nanometers. This bending is induced by the bimetallic effect as gold and titanium have different thermal expansion coefficients. This enables a normalisation of the mechanical signal from sensor to sensor. Normalisation coefficients for each individual cantilever are generated by dividing

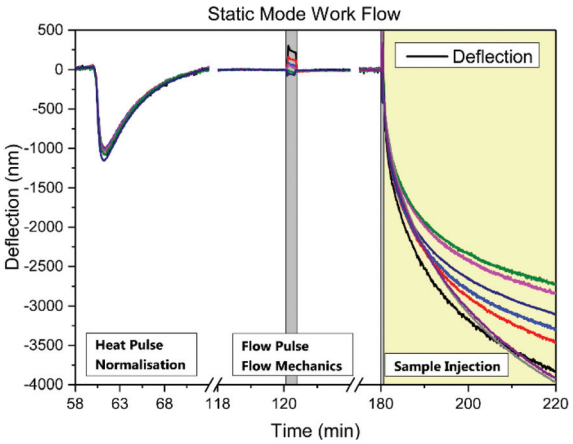

Fig. 5 Automated workflow of cantilever experiments. First, a temperature pulse (+2 °C) is induced at 60 minutes for 12 seconds to allow for subsequent mechanical normalisation between cantilevers in one array. The cantilevers bend depending on their individual bimetallic coating, a narrow distribution indicates mechanical conformity. Then, a flow pulse (38 μl at 150 μl min^{-1}) at 120 minutes as a control experiment reveals any flow induced motion. Laminar streaming causes the cantilevers deflection. The sensors should immediately come back to the base line after the flow pulse if the flow is not altering the mechanics of the sensor. Then 38 μl at 150 μl min^{-1} of miRNA containing samples are injected and the raw data of the sensors are recorded while the solution in the fluid chamber is again stopped (yellow background). White background indicates no flow, grey areas depict buffer flow and the yellow background illustrates sample incubation.

the average response of all 8 cantilevers to the heat pulse by the cantilevers individual response. Subsequently we introduced a dummy buffer injection with a flow of 38 μl at 150 μl min^{-1} (grey background) to observe fluidic effects during streaming. Since all experiments described in the following paragraphs are conducted in a stop/flow/stop condition, deflections caused by flow after a dummy buffer injection could be excluded when the sensors return to their stable baseline. Sample injection of 38 μl takes place when the cantilevers are stable post heat pulse. Incubation time in the chamber without liquid motion is 20 minutes (yellow background), allowing reactions to occur on the cantilevers surface. Sample is then removed by a 300 μl buffer wash at 150 μl min^{-1}. All events are controlled automatically, to ensure reproducibility and reduce user error. Raw data is baseline corrected before the injection event and multiplied by the individual normalisation coefficients. Cantilevers containing the same ssDNA probe surface coating (two per probe) are averaged. Following this, the mean reference sensor response is subtracted from the mean target sensitive response, giving a differential signal for each miRNA being individually targeted. Each data point taken is an average of 5000 points. Data points in Fig. 2 are mean values from three experiments for both cantilever array and SPR data.

SPR measurements

All SPR measurements were performed on a Biacore 2000 instrument (Biacore Life Sciences, GE Healthcare). A detailed

description of the chip preparation is shown in the ESI.† Before each injection we recorded a stable SPR baseline to ensure that the system was equilibrated. Samples of clean oligonucleotides in DPBS+ with concentrations between 1000 nM and 0 nM were injected in series with urea regeneration in between. Samples were diluted in 1 : 2 steps. The measurements were repeated three times per concentration measured.

Sample preparation (detection of miRNA in cell lysates or in blood plasma)

Cell Lysates from Huh7 cells (miR-122 positive) and Me15 cells (miR-122 negative, ESI Fig. S1†) were produced by cell culturing, lysing and centrifugation. Exact details of how the cell lysates were produced can be found in the ESI.† To study the effects on circulating miRNA induced by an APAP overdose *in vivo*, rats were exposed to 2 g kg^{-1} for 24 hours. Harvested blood was centrifuged and EDTA treated to generate plasma, subsequently stored at −20 °C. Prior to injection, 10 μl of plasma was expanded to 75 μl to ease sample handling. Control experiments (no APAP overdose) were also conducted in serum (Sigma R9759). Various miRNA extraction kits were tested with miRNA in H_2O and commercial serum. Unfortunately, none of the kits gave satisfactory quantitative results. The optimal approach was therefore to inject directly diluted plasma. Non-treated rat serum was diluted to the same protein concentration as the APAP treated rat plasma upon injection (502 μg ml^{-1}). Protein concentration was determined using a Bradford assay.[51]

Animal study (drug induced liver injury)

APAP induced liver injury is clinically relevant, well studied, and can be rapidly induced *in vivo* with a single dose, it has become a standard model in the pharmacology and toxicology literature. For all experiments, food was withdrawn 12–15 hours prior to treatment with APAP. The rats were treated orally with one 2 g APAP per kg body weight in metabolically inert vehicles (0.5% methyl cellulose) to observe induced DILI (usually 1–2 g per kg body weight). After 24 hours the animals (rats) were euthanized by exsanguination under anesthesia.[52] Blood was drawn from the caudal vena cava and centrifuged to obtain plasma.

Regulations concerning the use of animals in research were adhered to and the 3 Rs: Reduction, Refinement and Replacement – in animal related experiments are followed. Animal experiments were approved by Swiss authorities according to international animal protection guidelines.

Conflicts of interest

There are no conflicts to declare.

Acknowledgements

This work was supported by Science Foundation Ireland under the IvP scheme SFI/09IN/1B2623, the CSET scheme SFI/10/CSET/B1821 and the SFI/15/IA/3023. We also thank F. Hoffmann-La Roche Ltd for financial support. Funding from commercial sources does not carry any conflict of interest.

References

1 R. C. Lee, R. L. Feinbaum and V. Ambros, *Cell*, 1993, **75**, 843–854.
2 P. S. Mitchell, R. K. Parkin, E. M. Kroh, B. R. Fritz, S. K. Wyman, E. L. Pogosova-Agadjanyan, A. Peterson, J. Noteboom, K. C. O'Briant, A. Allen, D. W. Lin, N. Urban, C. W. Drescher, B. S. Knudsen, D. L. Stirewalt, R. Gentleman, R. L. Vessella, P. S. Nelson, D. B. Martin and M. Tewari, *Proc. Natl. Acad. Sci. U. S. A.*, 2008, **105**, 10513–10518.
3 J. D. Arroyo, J. R. Chevillet, E. M. Kroh, I. K. Ruf, C. C. Pritchard, D. F. Gibson, P. S. Mitchell, C. F. Bennett, E. L. Pogosova-Agadjanyan and D. L. Stirewalt, *Proc. Natl. Acad. Sci. U. S. A.*, 2011, **108**, 5003–5008.
4 N. Kosaka, H. Iguchi, Y. Yoshioka, F. Takeshita, Y. Matsuki and T. Ochiya, *J. Biol. Chem.*, 2010, **285**, 17442–17452.
5 A. Zernecke, K. Bidzhekov, H. Noels, E. Shagdarsuren, L. Gan, B. Denecke, M. Hristov, T. Köppel, M. N. Jahantigh and E. Lutgens, *Sci. Signaling*, 2009, **2**, ra81–ra81.
6 P. S. Chen, J. l. Su and M. C. Hung, *J. Biomed. Sci.*, 2012, **19**, 90.
7 A. Afshari, J. Schrenzel, M. Leven and S. Harbarth, *Crit. Care*, 2012, **16**, 222–234.
8 K. R. Cordes and D. Srivastava, *Circ. Res.*, 2009, **104**, 724–732.
9 L. Tan, J.-T. Yu, Q.-Y. Liu, M.-S. Tan, W. Zhang, N. Hu, Y.-L. Wang, L. Sun, T. Jiang and L. Tan, *J. Neurol. Sci.*, 2014, **336**, 52–56.
10 Y. Yamaura, M. Nakajima, N. Tatsumi, S. Takagi, T. Fukami, K. Tsuneyama and T. Yokoi, *Toxicology*, 2014, **322C**, 89–98.
11 G. Ostapowicz, R. J. Fontana, F. V. Schiødt, A. Larson, T. J. Davern, S. H. Han, T. M. McCashland, A. O. Shakil, J. E. Hay and L. Hynan, *Ann. Intern. Med.*, 2002, **137**, 947–954.
12 R. J. Temple and M. H. Himmel, *J. Am. Med. Assoc.*, 2002, **287**, 2273–2275.
13 B. V. Martin-Murphy, M. P. Holt and C. Ju, *Toxicol. Lett.*, 2010, **192**, 387–394.
14 X.-J. Huang, Y.-K. Choi, H.-S. Im, O. Yarimaga, E. Yoon and H.-S. Kim, *Sensors*, 2006, **6**, 756–782.
15 A. Bessa, M. Nissenbaum, A. Monteiro, P. G. Gandra, L. Nunes, A. Bassini-Cameron, J. P. S. Werneck-de-Castro, D. V. de Macedo and L.-C. Cameron, *Br. J. Sports Med.*, 2008, **42**, 889–893.

16 M. Macheret and T. D. Halazonetis, *Annu. Rev. Pathol.*, 2015, **10**, 425–448.
17 M. Li, J. Li, X. Ding, M. He and S.-Y. Cheng, *AAPS J.*, 2010, **12**, 309–317.
18 C. Théry, L. Zitvogel and S. Amigorena, *Nat. Rev. Immunol.*, 2002, **2**, 569–579.
19 G. Rabinowits, C. Gerçel-Taylor, J. M. Day, D. D. Taylor and G. H. Kloecker, *Clin. Lung Cancer*, 2009, **10**, 42–46.
20 S. Ono, S. Lam, M. Nagahara and D. S. Hoon, *Clin. Med.*, 2015, **4**, 1890–1907.
21 X.-J. Lin, Y. Chong, Z.-W. Guo, C. Xie, X.-J. Yang, Q. Zhang, S.-P. Li, Y. Xiong, Y. Yuan and J. Min, *Lancet Oncol.*, 2015, **16**, 804–815.
22 Z. Zhang, W. Zheng and J. Hai, *Med. Oncol.*, 2014, **31**, 984.
23 C. Coulouarn, V. M. Factor, J. B. Andersen, M. E. Durkin and S. S. Thorgeirsson, *Oncogene*, 2009, **28**, 3526–3536.
24 P. Landgraf, M. Rusu, R. Sheridan, A. Sewer, N. Iovino, A. Aravin, S. Pfeffer, A. Rice, A. Kamphorst, M. Landthaler, C. Lin, N. Socci, L. Hermida, V. Fulci, S. Chiaretti, R. Foa, J. Schliwka, U. Fuchs, A. Novosel, R. Muller, B. Schermer, U. Bissels, J. Inman, Q. Phan and M. Chien, *Cell*, 2007, **129**, 1401–1414.
25 S. Linsen, E. de Wit, E. de Bruijn and E. Cuppen, *BMC Genomics*, 2010, **11**, 249–260.
26 R. McKendry, J. Zhang, Y. Arntz, T. Strunz, M. Hegner, H. P. Lang, M. K. Baller, U. Certa, E. Meyer and H.-J. Güntherodt, *Proc. Natl. Acad. Sci. U. S. A.*, 2002, **99**, 9783–9788.
27 G. Oliviero, S. Federici, P. Colombi and P. Bergese, *J. Mol. Recognit.*, 2010, **24**, 182–187.
28 R. Mishra and M. Hegner, *Nanotechnology*, 2014, **25**, 225501.
29 J. Zhang, H.-P. Lang, F. Huber, A. Bietsch, W. Grange, U. Certa, R. McKendry, H.-J. Güntherodt, M. Hegner and C. Gerber, *Nat. Nanotechnol.*, 2006, **1**, 214–220.
30 P. Noy, R. Steiner, J. Voelkle, M. Hegner and C. Fattinger, *Sensors*, 2012, **2012**, 208079.
31 B. N. Johnson and R. Mutharasan, *Biosens. Bioelectron.*, 2012, **32**, 1–18.
32 H. H. Nguyen, J. Park, S. Kang and M. Kim, *Sensors*, 2015, **15**, 10481–10510.
33 Q. Wang, R. Liu, X. Yang, K. Wang, J. Zhu, L. He and Q. Li, *Sens. Actuators, B*, 2016, **223**, 613–620.
34 L. Zhang, J. Wang, J. Zhang, Y. Liu, L. Wu, J. Shen, Y. Zhang, Y. Hu, Q. Fan and W. Huang, *ACS Sens.*, 2017, **2**, 1435–1440.
35 F. Siegrist, T. Singer and U. Certa, *Biol. Proced. Online*, 2009, **11**, 113–129.
36 M. Ravon, M. Berrera, M. Ebeling and U. Certa, *RNA Biol.*, 2012, **9**, 87–97.
37 S. B. Patil, M. Vögtli, B. Webb, G. Mazza, M. Pinzani, Y.-A. Soh, R. A. McKendry and J. W. Ndieyira, *Nat. Nanotechnol.*, 2015, **10**, 899.
38 F. Huber, H. P. Lang, M. Hegner, M. Despont, U. Drechsler and C. Gerber, *Rev. Sci. Instrum.*, 2008, **79**, 086110.
39 N. V. Lavrik, M. J. Sepaniak and P. G. Datskos, *Rev. Sci. Instrum.*, 2004, **75**, 2229–2253.
40 H. P. Lang, M. Hegner and C. Gerber, *Mater. Today*, 2005, **8**, 30–36.
41 K. Wang, S. Zhang, B. Marzolf, P. Troisch, A. Brightman, Z. Hu, L. E. Hood and D. J. Galas, *Proc. Natl. Acad. Sci. U. S. A.*, 2009, **106**, 4402–4407.
42 M. Arrese, A. Eguchi and A. E. Feldstein, *Semin. Liver Dis.*, 2015, **35**(1), 43–54.
43 X. Li, S. U. Mertens-Talcott, S. Zhang, K. Kim, J. Ball and S. Safe, *Endocrinology*, 2010, **151**, 2462–2473.
44 B. Nelson, T. Grimsrud, M. Liles, R. Goodman and R. Corn, *Anal. Chem.*, 2001, **73**, 1–7.
45 A. I. K. Lao, X. Su and K. M. M. Aung, *Biosens. Bioelectron.*, 2009, **24**, 1717–1722.
46 J. A. Gonzalez-Masia and D. C. Garcia-Olmo, *OncoTargets Ther.*, 2013, **6**, 819–832.
47 K. S. Gustafson, *J. Mol. Diagn.*, 2008, **10**, 33–42.
48 M. Walther, P. M. Fleming, F. Padovani and M. Hegner, *EPJ Tech. Instrum.*, 2015, **2**, 1–24.
49 F. Padovani, J. Duffy and M. Hegner, *Anal. Chem.*, 2017, **89**, 751–758.
50 A. Bietsch, J. Zhang, M. Hegner, H. P. Lang and C. Gerber, *Nanotechnology*, 2004, **15**, 873.
51 M. M. Bradford, *Anal. Biochem.*, 1976, **72**, 248–254.
52 M. R. McGill, C. D. Williams, Y. Xie, A. Ramachandran and H. Jaeschke, *Toxicol. Appl. Pharmacol.*, 2012, **264**, 387–394.

Electronic Supplementary Material (ESI) for Nanoscale.

Supplementary Information

Towards personalised rapid label free miRNA detection for cancer and liver injury diagnostics in cell lysates and blood based samples

James Duffy[1], Francesco Padovani[1], Giulio Bruntetti[1], Peter Noy[2], Ulrich Certa[2,3], Martin Hegner[1,*]

[1] Centre for Research on Adaptive Nanostructures and Nanodevices (CRANN), School of Physics, Trinity College Dublin, Dublin 2, Ireland

[2] F. Hoffmann-La Roche Ltd., Pharma Research and Early Development, Discovery Technologies, 4070 Basel, Switzerland

[3] F. Hoffmann-La Roche Ltd., Global Non-clinical Safety, Molecular Toxicology, 4070 Basel, Switzerland

[*] Corresponding author: Email: martin.hegner@tcd.ie

Methods

Cantilever prototype device was designed and built according to Walther et al.[35] and Noy et al. [30] Presented below are further details regarding the technical aspects of the prototype device and experimental procedures. Preparation techniques for SPR chips and cantilever array sensor are detailed. The cell lysates preparation is also described.

Cantilever measurement device

Enhancements made to the device referenced in Walther et al. [35] are: (1) Larger surface area position sensitive detector (PSD) (1L20-20-A_SU9 SiTek Electro Optics), (2) Data acquisition board with higher sampling rate (PCIe-6361, National Instruments), (3) Improved thermoregulation system (miniStat 125, Huber Kaltemaschinenbau GmbH), (4) dual syringe pump with solutions and samples contained inside the thermoregulation system (neMESYS system, Cetoni GmbH). The entire experimental set up and data acquisition is controlled by custom made LabVIEW (Version 14.0.1f3 64-bit) software interface.

Cantilever Array Preparation

Vacuum deposition rates of 0.2 Å /s and 0.5 Å /s were used for titanium (3 nm) and gold (23 nm) respectively before being stored under argon. Thiolated ssDNA probes arrived in a protective 0.1mM dithiothreitol (DTT) solution. This DTT needed to be removed prior to functionalisation via liquid-liquid phase separation (4 times) using ethyl acetate (Sigma Aldrich). After DTT extraction probe solutions of 20 µM in 50mM trithylammonium acetate are stored under argon at -20 °C. All solutions were made with twice filtered (0.2µm), twice autoclaved nanopure H_2O.

Cantilever measurement protocol

After priming the device with DPBS+ buffer and sample, the chip was mounted into the measurement chamber. Laser focusing onto the tips of the cantilevers was performed automatically. Once the internal temperature has stabilised, the experiment begins by testing the cantilever mechanical response to a heat pulse of +2 °C above the stable set point and a flow pulse of 38 µl at 150 µl/min. The downward deflection observed during the heat pulse or peltier test is used to normalise the mechanical response of the cantilevers during analysis. Sample injection of 38 µl at 150 µl/min takes place when the cantilevers are stable post peltier test. Incubation time is 20 minutes, allowing reactions to occur on the cantilevers surface. Sample is then removed by a 300 µl buffer wash at 150 µl/min. All events are controlled automatically, to ensure reproducibility and reduce user error.

SPR chip preparation

As sensor chips, we used either recycled CM5 or SM Biacore sensor chips or commercially bought Biacore Au sensor chips (BR-1005- 42, Biacore AB, Sweden). To enable recycling the CM5 and SA chips were rinsed in and stored in PBS (Sigma Aldrich). Then the chip holder containing the chips was placed in Deconex 12PA (Borer Chemie AG, Switzerland) in an ultrasonic bath for 15 minutes at 50 °C. Following this, they were rinsed with and stored in nanopure water for 10 minutes. The chip holder was then filled with Deconex 20NS (Borer Chemie AG, Switzerland) and placed in an ultrasonic bath for 15 minutes at 50 °C. Finally, the chips and chip holder were rinsed with and stored in nanopure water for 30 minutes before drying with nitrogen gas flow. Prior to the functionalisation the chips were treated with UV/O_3 for 10 min. The SPR chip was functionalised outside the instrument. The ssDNA probes were

immobilized onto the surface by pipetting 50 µl of 10 µM thiolated ssDNA in 50 mM TEAA buffer. The solution was incubated on the chip overnight (**>**10 h). The chip was rinsed with TEAA buffer for 30 seconds, respectively 3 times with buffer. Afterwards the chip was incubated for 1 hour with 50 µl of 10 µM 11-Mercapto-1-undecanol (Sigma) solution. The chip was rinsed with H_2O 3 times 30 seconds and dried in an air-stream of N_2 then stored under Argon at 4 °C.

Cell sample preparation

1 ml cell stock of Huh7 or Me15 cells was seeded into cell culture flasks (BD Biosciences) with 10 ml Dulbecco's Modified Eagle Medium + 10% Fetal Bovine Serum medium (Gibco/Thermofisher). When the cells were fully confluent the flask was drained and washed with 5 ml DPBS+. The DPBS+ was then removed and 500 µl trypsin was added to the flask for 5 minutes incubation. Following this, 5 ml medium was added and the cells were transferred to a medium flask with 20 ml of medium. For transfer to larger flask 1 ml trypsin was used to dissociate the cells. In the large flask 4 ml of cell solution was added to 26 ml medium. Dissociation from the large flasks was performed using 2 ml trypsin after rinsing with DPBS+. Cells were aspirated into a falcon tube using 10 ml medium. An additional 25 ml of medium was then added to ensure the trypsin was inhibited. A cell count using 10 µl was performed. Two fractions of cell solution containing each 10 x 10^6 cells were transferred to two 15 ml falcon tubes. The tubes were centrifuged for 5 min at 400 rpm. Buffer was removed and the pellet was resuspended in 10 ml lysis-buffer (8 ml H_2O and 2 ml Lysis-buffer (Passive Lysis Buffer 5x, Promega)) to a final concentration of 10^6 cells/ml. Similar to serum samples the cell lysate was expanded from 10 µl to 75 µl (protein concentration upon injection was 28.3 µg/ml).

Direct cancer related miRNA detection in cell lysates

In the set of experiments presented here we performed control measurements on two cell lines investigated. Me15 cell lysate are miRNA-122 (target) negative while Huh7 cell lysate are miRNA-122 positive. The control cell lysate (Me15) produced a nanomechanical differential signal of 100 nm due to interference from background molecules. This offset serves as a baseline for Me15 miR-122 spike in experiment as shown in Fig. 2 of the main text. The specific annealing of the miRNA target in Huh7 cell lysate generates extra surface stress resulting in approximately 200 nm differential deflection indicating a target concentration of roughly 500 pM.

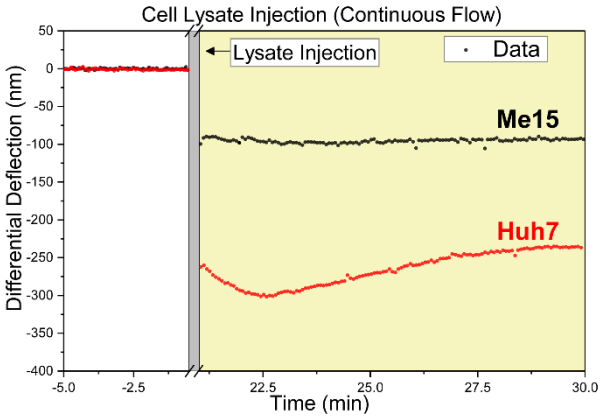

Figure S1. Overlay of two consecutive continuous flow experiments to investigate the detection of miR-122 in Me15 and Huh7 cell lysate: The graph shows the significant difference between the injection of miRNA-122 positive Huh7 cell lysate (red curve) and the injection of Me15 cell lysate (black curve) which is miR-122 negative. Two injections were performed in series on the same cantilever array chip. The line break (grey area) represents a series of fluidic events including sample introduction involving flow of 600 µl at 150 µl/min, 10 minutes of incubation and a buffer wash of 450 µl at 150 µl/min. Yellow area depicts sensor response post wash. Sample was not diluted resulting in particles scattering the optical signal

during incubation, creating fluctuations in the deflection reading. The reference sequence used was a firefly luciferase gene segment. miR-122 target sensitive cantilevers response are averaged form multiple cantilevers as is the reference response. Post fluidic events the Huh7 sample induces ~200 nm differential deflection whereas the injection of the negative control (Me15) leads to ~100 nm differential deflection signal. The response induced by the Me15 cell lysate is due to nonspecific interactions and is stable post wash while the Huh7 cell lysate response is greater post wash as miR-122 are present to occupy surface bound probes.

Surface plasmon resonance dose response

These experiments were performed on Biacore's surface plasmon resonance (SPR) system to establish a dose response curve for miRNA hybridisation. We utilized SPR chips with blank gold surfaces that were functionalised with oligonucleotides. Various concentrations of pure miRNA target were injected as background interference would mask the miRNA hybridisation signal. While the corresponding cantilever measurements were conducted in cell lysates. This data is summarized in Figure 2 of the main text.

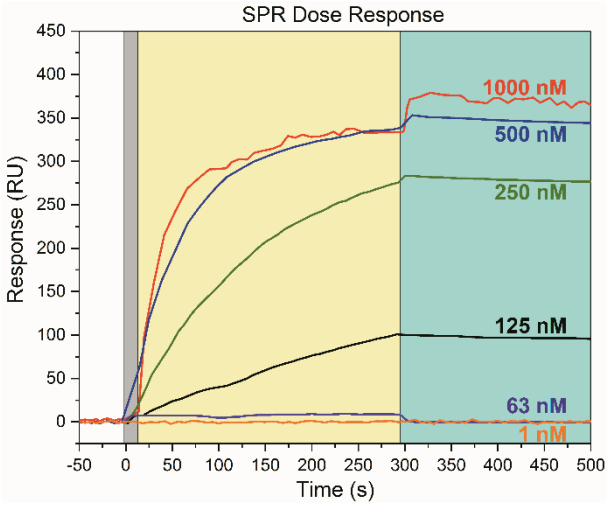

Figure S2. Overlay of multiple SPR hybridisation dose response experiments using Biacore sensor chip functionalised with 1 µM thiolated probe for 1 hour. Grey area represents 25 µl injection of pure miRNA target (various concentrations). Incubation is indicated by the yellow area and rinsing with PBS buffer at 25 µl/min is depicted in the blue area. The result value for each concentration was taken just after the rinse began as excess molecules which may interfere with the signal are removed. 1000 nM and 500 nM seem to reach saturation and therefore have similar amplitudes. Signals from lower concentrations are ambiguous.

Cantilever array dose response

These experiments were all performed on separate cantilever arrays with four target sensitive and four control cantilevers. Me15 cell lysates were spiked with various centration's of target miRNA. The sensor was then exposed to undiluted sample in flow through conditions. Following this a buffer rinse was performed to reveal the result.

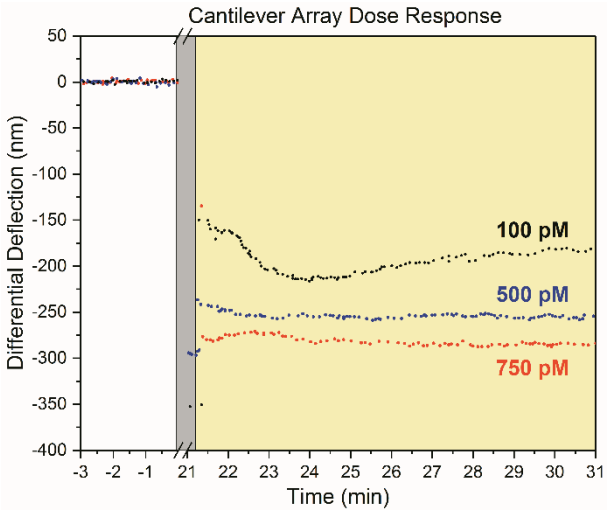

Figure S3. Overlay of multiple cantilever array dose response experiments. Cantilever array annealing data obtained from three miRNA target spike-in concentration experiments in Me15 cell lysate background in flow-through conditions. The line break (grey area) represents a series of fluidic events including sample introduction involving flow of 600 µl at 150 µl/min, 10 minutes of incubation and a buffer wash of 450 µl at 150 µl/min. Yellow area depicts sensor response post wash. Sample was not diluted resulting in particles scattering the optical signal during incubation, creating fluctuations in the deflection reading. The differential signal was created by subtracting the average response of four target (miR-122) sensitive cantilevers from the averaged response of four control sensors. A Differential signal from 100 pM non amplified target in undiluted cell lysates was achieved using the label free cantilever array diagnostic platform.